IEEE Access
Multidisciplinary | Rapid Review | Open Access Journal

SPECIAL SECTION ON UNCERTAINTY QUANTIFICATION IN ROBOTIC APPLICATIONS

Received April 12, 2020, accepted April 26, 2020, date of publication May 6, 2020, date of current version May 20, 2020.

Digital Object Identifier 10.1109/ACCESS.2020.2992567

Artificial Human Balance Control by Calf Muscle Activation Modelling

KAIYANG YIN[1,2,3], JING CHEN[1], KUI XIANG[1], MUYE PANG[1], BIWEI TANG[1], JIE LI[4], AND LONGZHI YANG[3], (Senior Member, IEEE)

[1]School of Automation, Wuhan University of Technology, Wuhan 430070, China
[2]School of Electrical and Mechanical Engineering, Pingdingshan University, Pingdingshan 467000, China
[3]Department of Computer and Information Sciences, Northumbria University, Newcastle upon Tyne NE1 8ST, U.K.
[4]School of Computing, Engineering and Digital Technologies, Teesside University, Middlesbrough TS1 3BX, U.K.

Corresponding author: Longzhi Yang (longzhiyang@northumbria.ac.uk)

This work was supported by National Natural Science Foundation of China, Grand number 61603284 and 61903286.

ABSTRACT The natural neuromuscular model has greatly inspired the development of control mechanisms in addressing the uncertainty challenges in robotic systems. Although the underpinning neural reaction of posture control remains unknown, recent studies suggest that muscle activation driven by the nervous system plays a key role in human postural responses to environmental disturbance. Given that the human calf is mainly formed by two muscles, this paper presents an integrated calf control model with the two comprising components representing the activations of the two calf muscles. The contributions of each component towards the artificial control of the calf are determined by their weights, which are carefully designed to simulate the natural biological calf. The proposed calf modelling has also been applied to robotic ankle exoskeleton control. The proposed work was validated and evaluated by both biological and engineering simulation approaches, and the experimental results revealed that the proposed model successfully performed over 92% of the muscle activation naturally made by human participants, and the actions led by the simulated ankle exoskeleton wearers were overall consistent with that by the natural biological response.

INDEX TERMS Muscle stretch reflex, calf muscle activation, standing control, exoskeleton control.

I. INTRODUCTION

The neuromuscular model provides an effective mechanism to support robust robotic control in addressing the uncertainty led by the environment, which forms an integral part of robotic bionic control research. Despite the increasingly intensive attention [1]–[3], the neural control mechanisms responsible for the formation and adaptation of calf muscle activation for human upright standing balance control are still not well understood [4]. Muscle activation change mechanisms have been developed to respond to variations in support surface perturbations through descriptive measures [5], [6]. However, it is difficult to interpret the recorded changes in muscle activation concerning neural control mechanisms, as the relationship between sensory inflow led by the upright standing perturbation and resulting muscle activation is still not well comprehended.

There are generally three groups of approaches to simulate the control mechanisms in the human neural system to respond to the perturbation in a standing position. The first group of approaches focus on fast responses using the muscle stretch reflex model in postural control [7], due to the short reflex loop and thus accordingly prompt response to unexpected external perturbations [8]. The muscle stretch reflexes can be encoded by the muscle spindle information, and the key mechanical behaviour can then be effectively explained by a positive feedback scheme [9], as demonstrated by the simulated walking gait without parameter interventions in the work of [10]. Regarding standing control, the angle and velocity of the ankle sway are the two most important inputs to the muscle stretch reflex model, as the calf muscle activation is mainly driven by these two factors [11]. Despite its rapid responses, the muscle stretch reflex model does not always generate accurate muscle activation signals, as reported in [12].

The second group of approaches use a feedback law on the centre of mass (CoM) to simulate the nervous system to generate the muscle activation value during human postural responses [5], [6]. In this case, the human body is modelled as a single-link inverted pendulum, with the CoM being the centre of the body, and the link length being the height of the body in a natural standing position. The inputs of the CoM-based feedback control include the displacement, velocity, and acceleration of the CoM, which are weighted by a

The associate editor coordinating the review of this manuscript and approving it for publication was Leo Chen.

feedback gain. Several temporal muscle activation generation approaches have been proposed using this system with a carefully designed signal-propagation time delay [5], [6], [13]. However, the experiments in real-world situations demonstrated a significant time delay of the CoM kinematics, due to the dynamic and uncertain environment, which forms a main challenge for the CoM-based feedback control approach [13].

The third group of approaches apply multi-sensory models to artificially control the human upright standing in an uncertain environment [14]. The commonly used sensors include vestibular sensor measuring the 'body in space' angles, somatosensory foot pressure receptors measuring the centre of pressure, and the ankle angle sensor measuring the body-foot angle. The external disturbances can then be estimated based on the sensed information through a multi-sensory fusion function; from this, the muscle response can be approximated based on the estimated disturbances. This group of approaches usually require a large number of sensors, which are sometimes very difficult to deploy in a real-world environment, in addition to the high computational complexity.

This paper proposes a new approach to produce accurate and timely calf muscle activation by simulating the natural neurological balance control system, to address the aforementioned challenges. The model was developed based on a representative situation of upright standing balance control on a moving vehicle. It is well accepted that the orientation and motion information derived from sensory systems are used by the musculoskeletal system to generate corrective actions by humans, in an effort to respond to the destabilizing effects of gravity and external perturbations to maintain the desired body orientation [15], [16]. Informed by the research in anatomy, this study artificially simulates a simplified version of natural neurological balance control consisting of only the lower central nervous system (LCNS) and advanced central nervous system (ACNS). Then, the CoM-based feedback model is adapted to act as the ACNS, and the muscle stretch reflex control serves as the LCNS, which jointly ensure the timeliness and accuracy of the proposed system. The outputs of these subsystems are combined through an aggregation function to simulate its biological peer.

The proposed approach was validated and evaluated by both biological and engineering simulation approaches. The biological approach recorded both the kinematic and calf muscle Electromyographic (EMG) signals, and then an optimization algorithm was employed to the kinematic data in order to find the optimal feedback gain and time delay to enable the model to optimally match the records from EMG. In the engineering simulation approach, the proposed integrated control model was applied to a robotic ankle exoskeleton control implemented using the OpenSim platform with the results compared with those led by the conventional muscle-tendon complex (MTC) model. The proposed integrated control model provides an effective approach to support robust exoskeleton control in addressing the uncertainty led by the environment. Both experiments confirm the effectiveness and efficiency of the proposed approach. The main contributions of this work are three fold: 1) proposing an integrated calf muscle activation model, 2) developing an artificial human balance control approach, and 3) applying the proposed model to robotic ankle exoskeleton control.

The rest of the paper is organized as follows. Sec. II reviews the technical background about the natural neurological control system, muscle stretch reflex, and CoM-based feedback model. Sec. III details the proposed integration feedback model. Sec. IV applied the proposed model to robotic ankle exoskeleton and assessed the proposed model with results analyzed. The paper is concluded in Sec. V with future work discussed.

II. BACKGROUND

The underpinning technical backgrounds, including the natural neurological balance control system, muscle stretch reflex model, and CoM-based feedback model, are reviewed in this section.

A. NEUROLOGICAL BALANCE CONTROL

The natural central nervous system (CNS) includes two major structures: the brain and spinal cord [17]. The brain consists of the cerebrum, the brain-stem, and the cerebellum, which are usually jointly referred to as the ACNS. It controls most of the activities of the body, by interpreting, integrating, and coordinating the information it receives from the sense organs, and making decisions as to the instructions sent to the rest of the body. The spinal cord is also often referred to as the LCNS, which is the centre for coordinating many reflexes and contains reflex arcs that can independently control reflexes.

Based on the neurological research, the ACNS and LCNS work together to jointly produce human balance control [18]. The sense organs of the ACNS combine all the inputs provided by the proprioceptive system, visual system and vestibular system, and the sensory receptors feedback which effectively estimates the human body motion states; then the ACNS produces the stimulus signals which are transmitted to muscle through efferent neurons for effective muscle actions. The main function of ACNS control in human postural responses is reinforcing the activation of calf muscle [19]. Specific to the calf muscle, the ACNS has long signal transmission time delays and thus a long control loop [5], [6].

The LCNS is mainly implemented through the muscle stretch reflex in human balance control. The sense organs of the muscle stretch reflex involve spindle organs and Golgi tendon organ. These organs detect the muscle spindle length offset, spindle contraction velocity, and muscle force information, which collectively produce the action instructions by the spinal cord. Efferent neurons transmit action instructions to the effector organ, i.e., the calf muscle for human standing control. In contrast to the ACNS, the LCNS is inherently short control loop [7], which can activate the calf muscle immediately after any perturbations taking in effect for human balance control [19].

The ACNS and LCNS control subsystems effectively work together for accurate and timely human balance control, and their contributions are governed by the sense organs [20]. In specific, the contributions from the two subsystems have a strong linear correlation; the reduction in the contribution from one subsystem will be accompanied by a corresponding increase in the contribution from the other subsystem.

B. MUSCLE STRETCH REFLEX MODEL

The muscle stretch reflex is a fast muscle contraction generation mechanism, in response to the stretch of the muscle that involves an afferent signal into the spinal cord and an efferent signal out to the muscle [21]. It is a monosynaptic reflex which provides automatic regulation of muscle spindle length. As for calf muscles, the stretch reflex links sensory information about ankle mechanics directly to the activation of the calf muscles via alpha motoneurons, bypassing the spinal inputs. The key mechanical behaviour can be effectively represented as a positive feedback reflex scheme.

1) SENSORY INFORMATION

The sensory information is motivated by the signals based on the muscle spindle length change and its contraction velocity [22]. This sensory information can be computed using the human ankle angle θ_{foot}, which is defined as the angle between the foot and the shank segment [23], as illustrated in Fig. 1(b). In particular, the calf muscle spindle length l_m is computed as:

$$l_m(t) = r_{foot}\,\rho(\sin(\theta_{foot}(t) - \theta_{\max}) - \sin(\theta_{ref} - \theta_{\max})) + l_{opt}, \tag{1}$$

where r_{foot} describes the attachment radius of calf muscle, ρ is a scaling factor representing the pennation angle of the muscle fiber, l_{opt} is an optimal length of the muscle spindle, l_m, at which the muscle can provide the maximum isometric force, θ_{ref} stands for the ankle reference angle at which $l_m = l_{opt}$, and $\theta_{\max}$ is a constant ankle angle value subject to $max(r_{arm}) = r_{foot}cos(\theta_{foot} - \theta_{max})$ with (θ_{foot}) being the human ankle angle and r_{arm} being the moment arm of calf muscle contractile force. From this, the muscle spindle contraction velocity, v_m, can be obtained via the time derivative of muscle spindle length value l_m.

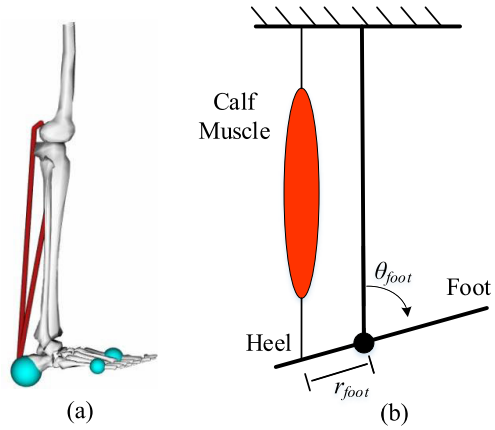

FIGURE 1. The ankle model (a) The ankle musculoskeletal model. (b) The simplified geometry of the muscle model skeletal attachment.

2) POSITIVE FEEDBACK REFLEX SCHEME

The calf muscle activation value, denoted as a_r, can be generated using the positive feedback reflex scheme [24], [25]. Denote the signal-propagation time delay as δ. The current muscle activation, $(a_r(t))$, at any time before δ is a_{r0}; otherwise, $a_r(t)$ is equal to the pre-activation a_{r0} plus a feedback component:

$$a_r(t) = \begin{cases} a_{r0}, & t < \delta \\ a_{r0} + p_l(l_m(t-\delta t) - l_o) + d_v v_m(t - \delta t), & t \geq \delta, \end{cases} \tag{2}$$

where p_l is the feedback gain for muscle spindle length offset, d_v represents the feedback gain for the muscle spindle length contraction velocity, and l_o expresses the muscle spindle length under muscle relaxation. The output muscle activation can then effectively simulate the muscle excitation-contraction coupling, and the resulting signal is constrained to the range between 0 and 1 [26].

C. CoM-BASED FEEDBACK MODEL

The CoM-based feedback model is another scheme to imitate the nervous control system for human upright standing control [5], [6], [13]. In this model, a common set of feedback signals related to horizontal CoM trajectories are used as the temporal formation of muscle activation.

1) CENTER OF MASS CALCULATION

In physics, the CoM of a body in space is the unique point where the weighted relative position of the distributed mass sums as zero. In human postural control, when body segments are in motion, the CoM of the body is continuously changing along time. Therefore, it is necessary to recalculate CoM regularly, which requires the knowledge of the trajectories of the CoMs of body segments. The CoM coordinate of each body segment CoM_i can be expressed as:

$$CoM_i = X_{di} + P_{CoMi}(X_{pi} - X_{di}), \tag{3}$$

where i stands for the i-th body segment, X_{di} and X_{pi} express distal end coordinate and the proximal end coordinate of the body segment, respectively, and P_{CoM_i} is a ratio of the distance between the CoM_i and X_{di} to the length of the i-th body segment.

By simplifying the human body as an n-segment system, the CoM of the body can be calculated as:

$$CoM_t = \frac{\sum_{i=1}^{n} m_i CoM_i}{M}, \tag{4}$$

where $M = \sum_{i=1}^{n} m_i$ is the total mass of the body, m_i and CoM_i are the mass and the CoM coordinates of the i-th body segment, respectively.

2) CoM-BASED FEEDBACK SCHEME

The CoM-based feedback scheme represents an explicit formulation of temporal calf muscle activation (a_p), with overlapping contributions of body CoM trajectories horizontal displacement (p_c), velocity (v_c), acceleration (a_c), and a signal-propagation time delay (λ) [5]. In specific, the muscle activation at any time before λ is approximated as the pre-activation value (a_0); otherwise, the muscle activation (a_p) is formed by the weighted summation of the kinematic signals at time $(t-\lambda)$ based on the feedback gain $[k_p, k_v, k_a]$ plus the pre-activation (a_0):

$$a_p(t) = \begin{cases} a_{p0}, & t < \lambda \\ a_{p0} + k_p p_c(t-\lambda) + k_v v_c(t-\lambda) & \\ \quad + k_a a_c(t-\lambda), & t \geq \lambda. \end{cases} \tag{5}$$

The values of kinematic signal feedback gain $[k_p, k_v, k_a]$ and the signal-propagation time delay (λ) are specific to each participant and muscle. The reconstructed muscle activation (a_p) is half-wave rectified, and constrained to the range between 0 and 1.

III. ARTIFICIAL CALF MUSCLE ACTIVATION

The proposed calf muscle activation model is an artificial implementation of the neurological balance control as introduced in Sec. II-A, with the human balance control on a moving vehicle as an example throughout the paper for description. Accordingly, the proposed model consists of two key subsystems, including a CoM-based feedback model simulating the ACNS in the natural subsystem, and a muscle stench reflex model representing the LCNS. The CoM of a distribution of mass in space is a key point to describe and predict the human body motion, and thus it can be effectively used to simulate the functions of sense organs in the ACNS. The muscle stretch reflex produces fast muscle contraction control in response to stretches within the muscle, which is thus a representation for the LCNS subsystems. Similar to their natural biological counterparts, the combination of CoM-based feedback model and muscle stretch reflex complement each other, in producing fast but accurate activation signals for the calf muscle to support human standing control in an unstable or uncertain environment.

A. MODEL OVERVIEW

The framework of the proposed artificial calf muscle activation model is illustrated in Fig. 2, with the vehicle platform acceleration and deceleration in this work to simulate various perturbations. In particular, there are two control loops in parallel, with the CoM-based feedback model and the muscle stretch reflex model being the main components of the two loops. The two models take different information regarding the human's postural states as inputs; the outputs of these two models are combined through an aggregation function, which is then sent to the human model as the calf muscle activation value for human standing control.

The data flow in the control loops guarantees the strong complementarity of the proposed model in producing accurate and fast actions. The inputs of the CoM-based feedback model are human kinematic information collected using a motion capture system; and it firstly calculates the CoM displacement, velocity, and acceleration $[p_c, v_c, a_c]$ which are subject to a time delay (λ) to simulate the neural transmission and processing time. The output of the CoM-based feedback model is the reconstructed muscle activation (a_a), which is a weighted linear combination of the delayed CoM signals with the feedback gain $[k_p, k_v, k_a]$ used as the weights.

The muscle stretch reflex model takes the ankle angle deviation and its change rate $[\Delta\theta, \Delta\dot{\theta}]$ as inputs, which are also collected by a motion capture system. The model first calculates the muscle spindle length and its contraction velocity $[l_m, v_m]$. Subject to a time delay δ, the intermediate outputs are weighted by the reflex gains $[G_l, G_v]$ on each channel to reconstruct the subsystem output, i.e., the muscle

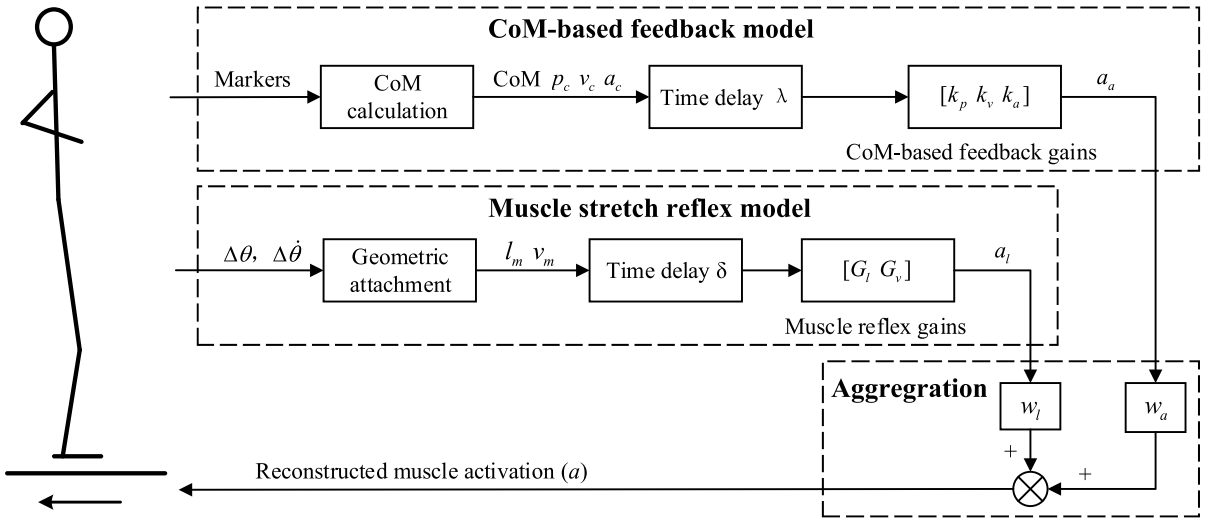

FIGURE 2. The framework of artificial calf muscle activation model for human upright standing control on a moving vehicle.

activation (a_l). Form this, the overall reconstructed muscle activation (a) is the aggregated output of a_a and a_l.

B. MUSCLE STRETCH REFLEX MODEL SUBSYSTEM

The muscle stretch reflex model firstly calculates the muscle spindle length l_m and the muscle spindle contraction velocity v_m as illustrated in Fig. 2. The muscle spindle length l_m is calculated based on the ankle angle deviation, as detailed in Sec. II-B.1. For the task of human upright balance control, the ankle angles θ_{foot}, i.e, the swing amplitudes, are usually small, that is $sin(\theta_{foot} - \theta_{\max}) \approx \theta_{foot} - \theta_{\max}$. According to Eq. 1, the calf muscle spindle length l_m can be expressed as:

$$l_m(t) = K(\theta_{foot}(t) - \theta_{\max}) + C, \tag{6}$$

where $K = r_{foot}\rho$ denotes a constant gain, and $C = -K\sin(\theta_{ref} - \theta_{\max}) + l_{opt}$ represents another constant. Thus, it can be approximated that the calf muscle spindle length is linearly correlated with the human ankle angle θ_{foot}.

The muscle spindle contraction velocity, v_m, can be calculated by the time derivative of the muscle spindle length value as:

$$v_m(t) = K\dot{\theta}_{foot}(t). \tag{7}$$

In other words, the calf muscle spindle contraction velocity can be calculated from the human ankle change rate, and there is a linear correlation between them.

According to the positive feedback reflex scheme in muscle stretch reflex model as discussed in Sec. II-B.2, the muscle activation produced by the model can be expressed as:

$$a_l(t) = p_l(l_m(t-\delta) - l_o) + d_v v_m(t-\delta), \tag{8}$$

where p_l and d_v represent the gain for muscle spindle length change and muscle spindle length contraction velocity, respectively, l_o describes the muscle spindle length under muscle relaxation. The value of l_o is taken as the muscle spindle length during the human standing equilibrium state in this work. By applying Eqs. 6 and 7, Eq. 8 can be re-expressed as:

$$\begin{aligned} a_l(t) &= p_l K(\theta_{foot}(t-\delta) - \theta_o) + d_v K(\dot{\theta}(t-\delta) - \dot{\theta}_o) \\ &= G_l\Delta\theta(t-\delta) + G_v\Delta\dot{\theta}(t-\delta), \end{aligned} \tag{9}$$

where $G_l = p_l K$, $G_v = d_v K$, and $\Delta\theta(t-\delta) = \theta_{foot}(t-\delta) - \theta_o$, and θ_o is the ankle angle in human standing equilibrium state. In particular, G_l and G_v correspond to the muscle reflex gains for ankle angle change and ankle angle change velocity, δ is the time delay caused by the neural transmission and information processing in muscle stretch reflex model. These parameters can be empirically determined based on the shape of the human body.

C. CoM-FEEDBACK MODEL SUBSYSTEM

The CoM-feedback model is used to reinforce the activation of the calf muscle to complement the muscle reflex model for human upright standing balance control. The inputs of the CoM-feedback model are the sensed information regarding the CoM trajectories, as discussed in Sec. II-C.

According to the CoM-based feedback scheme, the muscle activation led by the CoM-feedback model can be calculated by:

$$a_a(t) = k_p p_c(t-\lambda) + k_v v_c(t-\lambda) + k_a a_c(t-\lambda), \tag{10}$$

where p_c, v_c, and a_c are the horizontal displacement, velocity, and acceleration of the body CoM trajectories, respectively; k_p, k_v, and k_a correspond to the feedback gains for p_c, v_c, and a_c respectively, and λ is the time delay led by the neural transmission and information processing in CoM-based feedback model. These parameters, along with the parameters G_l, G_v, and δ used in the muscle stretch reflex module subsystem, can be globally optimised using a general optimisation approach, which will be discussed in Sec. III-E.

These CoM signals can be obtained from human kinematic markers. The kinematic markers are attached to the distal end and proximal end of the human body segments, i.e., the joints and ends of body segments; and the coordinate data of the markers are usually collected by a signal receiver in the motion capture system. The location of CoM and the mass of human body segment can then be obtained based on the anthropometric study [27]. From this, the CoM coordinate of the human body can be calculated using Eqs. 3 and 4, as detailed in Sec. II-C.1. From this, the CoM horizontal displacement can be calculated by:

$$p_c(t) = CoM_t(t) - CoM_0, \tag{11}$$

where $CoM_t(t)$ is the current CoM horizontal coordinate value, and CoM_0 is the CoM horizontal coordinate value during the human standing equilibrium state. The CoM horizontal velocity (v_c) is the first derivative of the CoM horizontal displacement (p_c) over time, and the CoM horizontal acceleration (a_c) is the second derivative of CoM horizontal displacement (p_c) versus time.

D. ACTIVATION AGGREGATION

The activation results from the two sub-systems should be aggregated to produced the final output. Information aggregation has been well studied in the literature, with many complex aggregation approaches being proposed, such as, Bayes estimation [28], fuzzy inference [29], neural network [30] amongst others. These complex aggregation approaches all involve uncertainty handling by introducing many parameters. Given that the proposed artificial calf muscle activation model has already included several parameters representing the uncertainty which are globally optimised as discussed in Sec. III-E, such as CoM-feedback gains and muscle stretch reflex gains. In order to avoid duplicating uncertainty management, this work takes the simplest weighted summation as the information aggregation approach, although the adaptation on the aggregation approaches, such as use the work reported in [31] and [32] remain as future work. Without losing generality, given any time t, the calf muscle activation

is defined as:

$$a(t) = \begin{cases} a_0, & 0 \leqslant t < \delta \\ a_0 + w_l a_l(t), & \delta \leqslant t < \lambda \\ a_0 + w_l a_l(t) + w_a a_a(t), & \lambda \leqslant t, \end{cases} \quad (12)$$

where a_0 represents the pre-activation value, δ and λ indicate the signal propagation delays for the two sub-systems, w_l and w_a are the weights of the results from the two sub-systems a_a and a_l, respectively. The current calf muscle activation ($a(t)$), at any time before δ is equal to the pre-activation value (a_0); at the time between δ and λ, $a(t)$ equals to a_0 plus the weighted activation from the muscle stretch reflex model, i.e., $w_l a_l(t)$; otherwise, the activation value is the combination of the pre-activation and the activations led by both sub-systems.

The weights are determined by the sensory information of the two sub-systems. By using the simple weighted summation, any reduction of the contribution from one subsystem will be accompanied by a corresponding increase in the contribution from the other subsystem [20], and the CoM trajectories horizontal velocity (p_v) and the muscle spindle length (l_m) are the primary sensory information used for weight determination in this work. Therefore, $[w_a, w_l]$ are designed to be linearly correlated with p_v and l_m, and their normalisations are used as the weights:

$$w_a = \frac{P}{P+L}, \quad (13)$$

$$w_l = \frac{L}{P+L}, \quad (14)$$

where P and L represent the normalisation of the horizontal velocity p_c of CoM trajectories, and the normalization of muscle spindle length l_m, respectively, that is:

$$P = \frac{p_v}{max(p_v)}, \quad (15)$$

$$L = \frac{l_m}{max(l_m)}. \quad (16)$$

E. FEEDBACK GAINS OPTIMIZATION

The parameters, such as the feedback gains $[G_l, G_v]$, $[k_p, k_v, k_a]$ and the signal-propagation time delay $[\delta, \lambda]$, vary for different muscles in different environments. These seven parameters can be globally optimised using a generic optimisation algorithm, with the covariance matrix adaption-evolution strategy (CMA-ES) being adopted in this work. Briefly, the CMA-ES uses a Gaussian distribution to sample the solution space of the optimisation problem, which is fitted by a number of iterations of updating guided by a fitness function [33].

The CMA-ES first initialises the parameters randomly within their universes of discourse. For artificial calf muscle activation, the feedback gains should be positive and the time delays must be restricted as $20ms < \delta < 80ms$ and $60ms < \lambda < 180ms$, [4], [34]. Then, the individuals of the first generation are sampled according to a multivariate Gaussian distribution, characterized by a mean vector (m) which was formed by the initialised parameters, a covariance matrix (C) and a standard deviation (d):

$$x^{(1)} \sim m^{(1)} + N(0, dC^{(1)}), \quad (17)$$

where $C^{(1)}$ is set as the identity matrix of order seven, and d is set to 1. Using the same approach, the population including γ individuals of the first generation can be generated.

The variance-accounted-for (VAF) is an indicator to assess the fitness of the reconstructed muscle activation in reference to the recorded muscle activation during the training stage [4], which is adapted in this work for individual evaluation. The VAF is defined as:

$$\%VAF = 100(1 - \frac{var(a - \hat{a})}{var(a)})\%, \quad (18)$$

where $var(\cdot)$ stands for the variance operation, and $\hat{a}$ is the reconstructed or predicted muscle activation value. With the support of this fitness function, all the individuals in the first generation can be ranked as: $x_1^g, \ldots, x_\gamma^g$, where $g = 1$ represents the first generation.

Then the top ranked μ individuals (i.e., parameter sets) are selected to produce the next generation mean vector by a weighted average function:

$$m^{(g+1)} = \sum_{i=1}^{\mu} w_i x_i^{(g)}, \quad (19)$$

where w_i denotes the positive weight coefficient. In this work, $\mu = \gamma/2$ and $w_i = 1/\mu$. Meanwhile, the selected individuals and the change in the mean vector are used to update the covariance matrix of the next generation:

$$C^{(g+1)} = \sum_{i=1}^{\mu} w_i (x_i^{(g)} - m^{(g)})(x_i^{(g)} - m^{(g)})^T. \quad (20)$$

After update the mean vector and covariance matrix, the population of the next generation are sampled according to a multivariate Gaussian distribution as expressed in Eq. 17, and can be expressed as:

$$x^{(g+1)} \sim m^{(g+1)} + N(0, dC^{(g+1)}). \quad (21)$$

This process is repeated from generation to generation to imitate the natural selection process, until a pre-defined threshold of fitness is reached. From this, the mean of the final calculated generation serves as the best estimate of the optimal parameter values.

IV. EXPERIMENTATION

The proposed artificial calf muscle activation model was evaluated in this section using a moving vehicle as the environment, by both biological and engineering approaches. The biological approach compared the reconstructed value of the calf muscle activation using the humanoid kinematics signals through the proposed model with that recorded from the postural responses of human participants. The engineering simulation approach applied the proposed model with the MTC to a robotic ankle exoskeleton control. In particular, the artificial

calf muscle activation model was used to calculate the muscle activation for the MTC, and then the MTC produces appropriate muscle force to counteract the environmental perturbation. All the data was processed with Matlab in this work.

A. BIOLOGICAL APPROACH

1) PARTICIPANTS

Five healthy participants from Wuhan University of Technology, aged 22.8 ± 1.47 years, height 1.73 ± 0.063m, weight 65 ± 7.6kg (representing mean ± standard divination), were recruited in this study. All participants signed an informed consent form before participating, and all collected data are anonymised.

2) EXPERIMENTAL PROTOCOL

A Nokov motion capture system (produced by Beijing Nokov Science & Technology Co., Ltd. China) with eight charge-coupled device cameras was employed for the vehicle kinematic data capturing. The camera system calibration and three-dimensional target reconstruction were performed by NK-cortex software (produced by Nokov, China). The vehicle kinematics were derived from 4 markers attached on the vehicle, and the participants kinematic were derived from 21 markers pasted on the joints of body-segments including head-arms-trunk, thigh, and shank-foot segments. The vehicle kinematic data were acquired at the frequency of 100Hz.

The calf includes two main muscles, i.e., the Gastrocnemius (Gas) and Soleus (Sol). Muscle activation from these two muscles was recorded using a surface electromyography (sEmg) acquisition instrument (DataLog MWX8, Biometrics, Ladysmith, VA, USA) with pairs of 3.0cm surface electrodes spaced 2 $\sim$ 4cm. The sampling frequency of the sEmg was 1000Hz, with differential amplification (gain: 1000) and common-mode rejection (104dB). Maximum Voluntary Contraction (MVC) tests were performed before the experimentation and then used for muscle activation signal normalization. The experimental setup is shown in Fig. 3.

During the data collection process, the participants were asked to maintain a standing position on a movable vehicle. The participants were instructed to cross their arms at the chest level, look straight ahead and react naturally while the vehicle was moving. Note that the vehicle was only able to move in the horizontal direction e.g. forward and backward in this experiment. An example of the recorded vehicle kinematic information (i.e., position, velocity, acceleration), human body kinematic information (i.e., CoM position, CoM velocity, CoM acceleration), and the calf muscle activation (i.e., Gas and Sol) are shown in Fig. 3. This experiment studies the participants' responses to the vehicle backward perturbations (the opposite direction that participants face), and five trials were collected from each participant.

Each trial lasted 2000ms. The muscle activation was calculated from the raw sEmg signals, where a high-pass filter with a cutoff frequency of 25 Hz (fourth-order zero-lag Butterworth filter) was applied to remove the DC offsets, and a low-pass filter with a cutoff frequency of 35 Hz (fourth-order zero-lag Butterworth filter) was applied to rectify. The process was adapted from the work reported in [4] where more details are available. The horizontal displacements of the participants' CoM motion trajectories were calculated from recorded kinematic data using a weighted sum of the segmental centre of masses, as detailed in Sec. II-C. In addition, the horizontal velocity and acceleration of the CoM trajectories were obtained via the derivation and second derivation of CoM displacement versus time, respectively. The parameters of the proposed model for Gas and Sol were optimised, as detailed in Sec. III-E, and the initial parameter values were set as $[G_l, G_v] = [0.1, 0.01]$, $[k_p, k_v, k_a] = [0.1, 1, 0.1]$, $[\delta, \lambda] = [20, 50]$ in this experiment. The optimised parameters settings are summarised in Figs. 4 and 5.

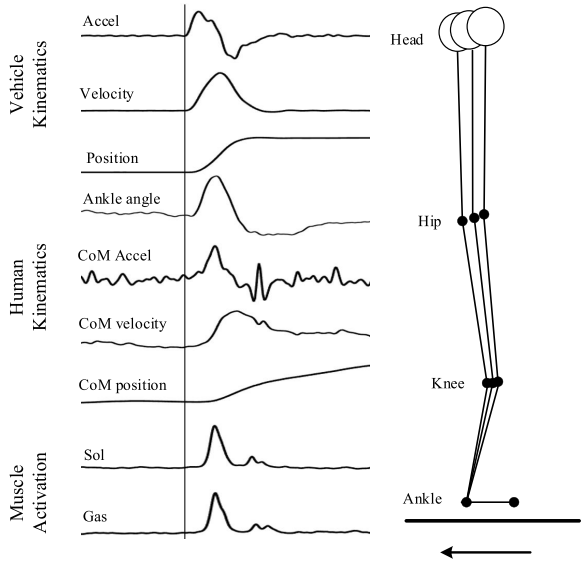

FIGURE 3. The experimental protocol and an example of human upright standing response.

3) EXPERIMENTAL RESULTS

Taking one of the trails by participant A as an example, the relationship between the ankle joint angle, the ankle joint angular velocity, the recorded CoM displacement trajectories, the recorded CoM velocity, the recorded CoM acceleration, the activation of Gas muscle and the activation of Sol muscle are illustrated in Fig. 6. Each trial was started by a participant standing on a static vehicle with an upright position. When the vehicle was triggered by a backward moving, the participant leaned forward naturally (as indicated by the black solid line in Fig. 6), and the ankle angle increased quickly along with the ankle angular velocity, as shown in Figs. 6 (a) and (b). It usually took about 300 $\sim$ 400ms to terminate the leaning forward phase and then changed to lean backward activities, after around another 400ms, the body of the participant established the equilibrium position. Compared with the upright position, the peak ankle angle increased about 4° and the peak

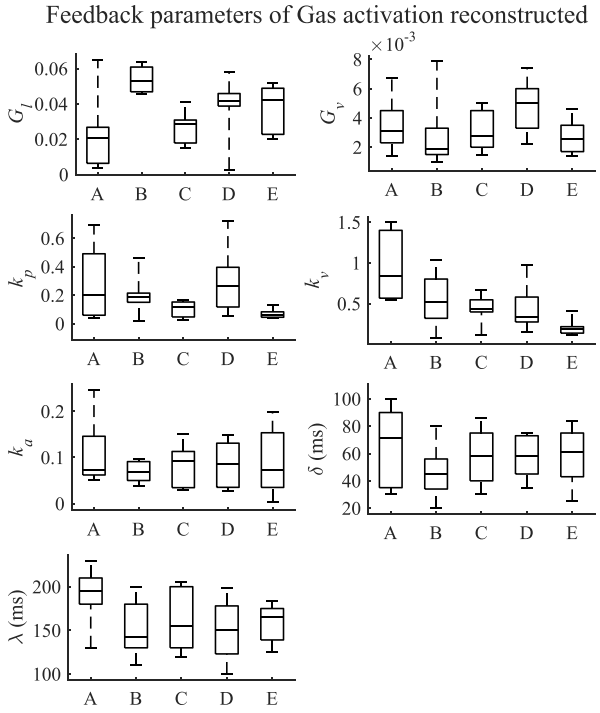

FIGURE 4. The variations in artificial calf muscle activation model parameters for predicting Gas muscle activations. The abscissa values A∼E represent the results of multiple trials for participants A∼E, respectively.

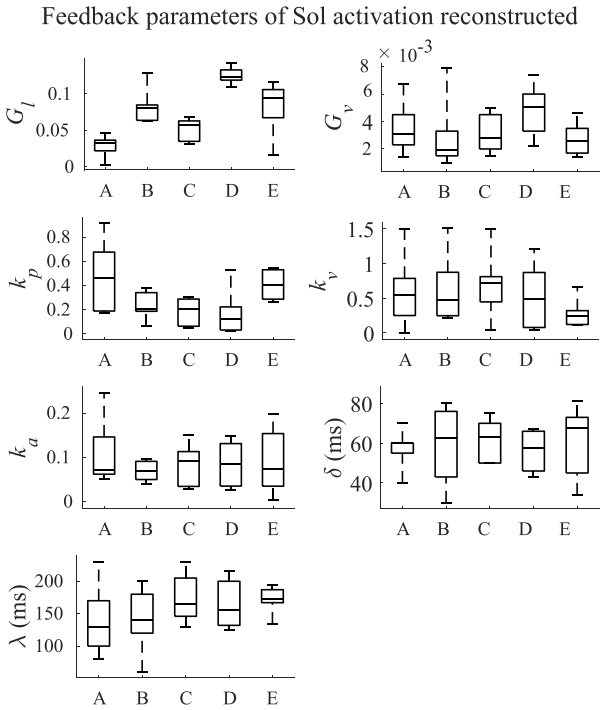

FIGURE 5. The variations in artificial calf muscle activation model parameters for predicting Sol muscle activations. The abscissa values A∼E represent the results of multiple trials of participants A∼E, respectively.

ankle angular velocity was $19°/s$ in the equilibrium position. In addition, a rise of the ankle angle consequently led the participant total CoM displacement also demonstrated,

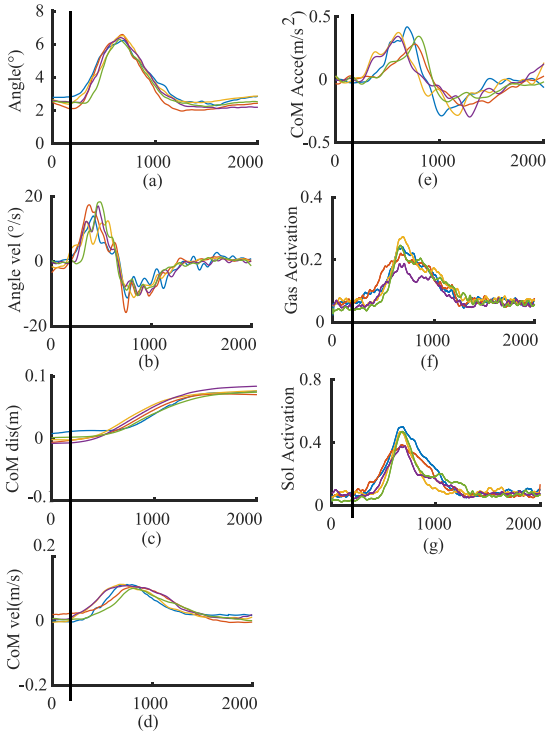

FIGURE 6. The experimental kinematic trajectories and muscle activation for participant A. Each colour denotes one trial in 2s, the black solid straight lines denote the time point when the vehicle started to move. (a): the ankle joint angle; (b): the ankle joint angular velocity; (c): the recorded CoM displacement trajectories; (d): the recorded CoM velocity; (e): the recorded CoM acceleration; (f): the activation of Gas muscle; and (g): the activation of Sol muscle.

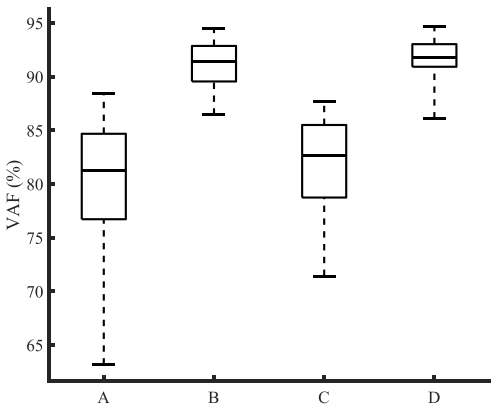

FIGURE 7. The variations in VAF for predicting calf muscle activation. Boxes delimit the middle 50% of the data, with the centre lines indicating the median value, and whiskers delimit the full range of the VAF value. A: Variations in the VAF value of reconstructed Gas activation led by the conventional muscle stretch reflex model to recorded activation; B: Variations in VAF value of Gas activation as reconstructed under the proposed model; C:Variations in VAF value of reconstructed Sol led by the conventional muscle stretch reflex control model; D: Variations in the VAF value of reconstructed Sol under the proposed model.

as confirmed by Fig. 6 (c). Unlike the CoM displacement, which was monotonically increasing, both CoM velocity and the CoM acceleration experienced a fluctuation in the range of $0 \sim 0.12m/s$ and $-0.3 \sim 0.4m/s^2$, as demonstrated in Figs. 6 (d) and (e), respectively. In terms of the Gas and Sol

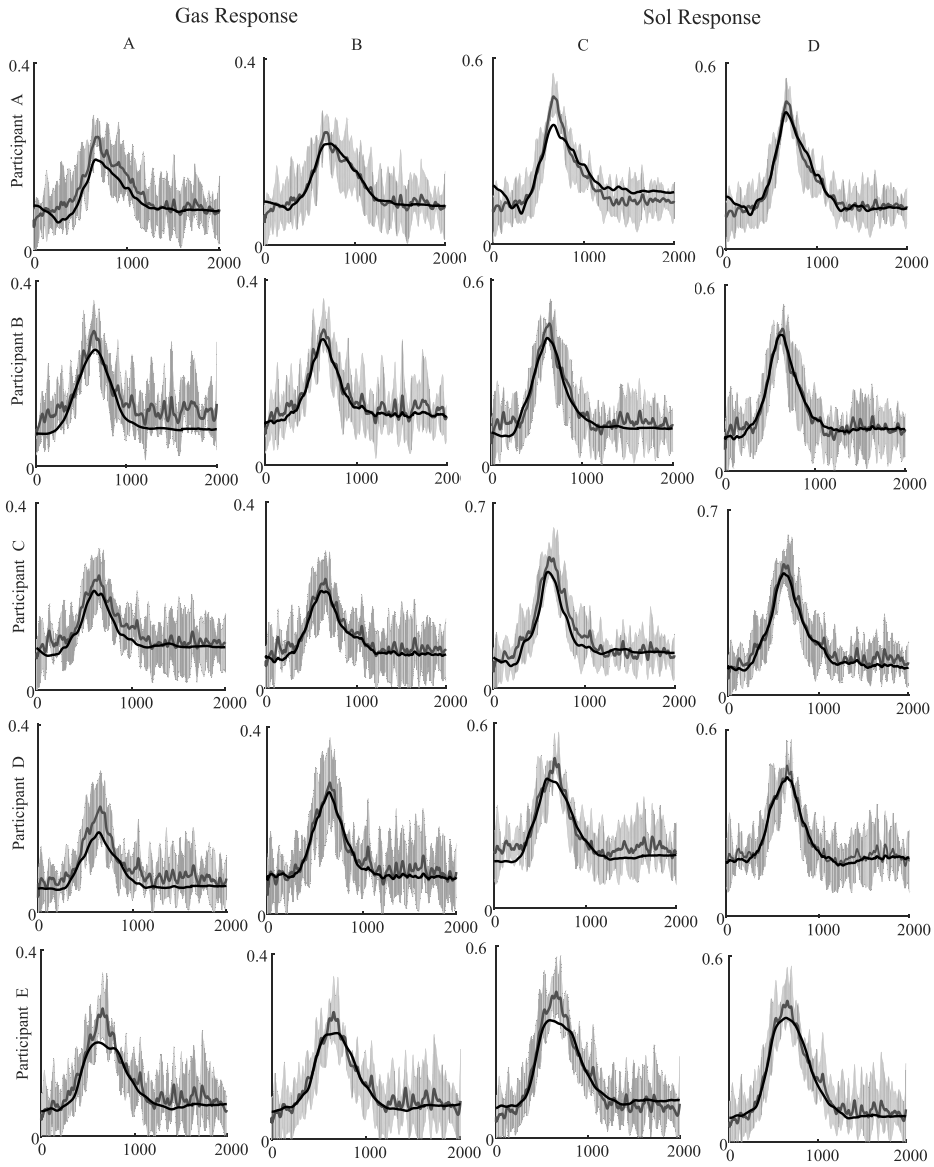

FIGURE 8. The averaged time courses of recorded (solid grey) and prediction (solid black) of calf muscle activations during upright standing responses, and the grey-shaded regions indicate SD from the mean recorded activations for each muscle across all five trials. All the prediction muscle activations were reconstructed with their respective optimal model parameters. A: Gas response activation led by the conventional muscle stretch reflex model control; B: Gas response activation under the proposed artificial calf muscle activation model; C: Sol response activation led by the conventional muscle stretch reflex model control; D: Sol response activation under the proposed artificial calf muscle activation model.

activation, under the control of the nervous system, the muscle activation of Gas and Sol got corresponding responses to counteract perturbation-induced postural sway, as shown in Figs. 6 (f) and (g). This phenomenon appeared in all five participants' trials. The reason for this response is that the vehicle moving brought horizontal perturbation, and the participants leaning let the humanoid gravity get rotation torque, then calf muscle should produce appropriate rotation torque to let the participant recover back to the equilibrium position.

The temporal patterns of calf muscle activation response to the vehicle moving perturbation for all five participants were reconstructed by both the proposed model and the conventional muscle stretch reflex model, for a comparative study. The comparison results are illustrated in Fig.8, where Figs. 8 - A & C indicate the response activation led by the conventional muscle stretch reflex model and Figs. 8 - B & D represent the response activation generated by the proposed model. It is clear that the muscle activation reconstructed by the proposed model in both Gas and Sol delivered better performances than the muscle activation reconstructed by the conventional muscle stretch reflex control model, as the activation generated by the proposed model better matches the ground truth, i.e. the human participants' natural response. For a better illustration, the Variance-Accounted-For (VAF) values were calculated to assess the fitness of the reconstructed muscle activation in reference to the ground

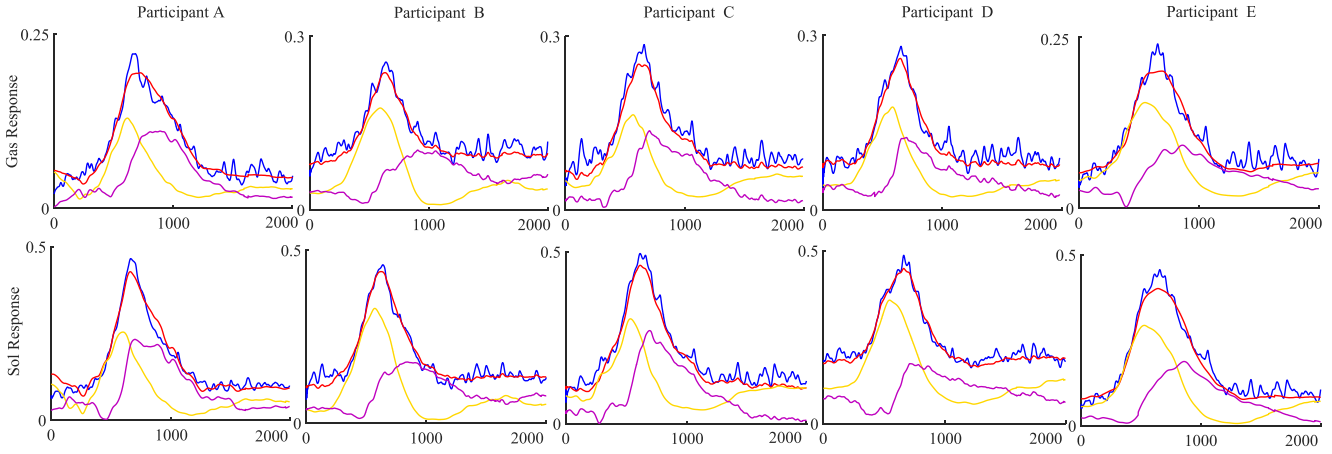

FIGURE 9. The contributions of each muscle to the time course for each participant. The blue solid lines represent the recorded muscle activation; the red solid lines indicate the reconstructed muscle activation led by the artificial calf muscle activation model; the yellow solid lines show the muscle stretch reflex model control subsystem contributions; and the purple solid lines demonstrate the CoM-feedback model subsystem contributions.

truth. The variation of the VAF and the mean of the VAF for both the conventional muscle stretch reflex model and the proposed model are shown in Fig. 7. In particular, the mean of the VAF for both Gas and Sol reconstructed by the conventional muscle stretch reflex control model is 82%, and the mean of the VAF for both Gas and Sol led by the proposed model is 92%.

In order to enable a direct comparison, a decomposition of the reconstructed muscle activation was performed to calculate the contributions of two muscles, i.e., Gas and Sol, as plotted in Fig. 9. The figures show that there are around 100∼200ms delays between the CoM-feedback model subsystem contributions (demonstrated in purple solid line) and muscle stretch reflex model subsystem (shown in yellow solid line) for all five participants. The reason is that the kinematic trajectories of body CoM variation are later than ankle angle variation for the vehicle moving perturbations. The influence on human standing upright balance control from the vehicle moving perturbation is a bottom-up process and the position of human CoM is higher than the ankle, which led to a long transmission distance and period between the human CoM and the perturbation from the moving vehicle than that between the ankle and the perturbation of the vehicle. Therefore, there is a delay of the effect of the perturbation on human CoM in reference to that on the ankle.

The determined weight of two subsystems for the activation aggregation (w_l and w_a) are also illustrated in Fig. 10. According to this figure, the weight values for the muscle stretch reflex model subsystem (w_l) was increased to the peak (from 0.65 to 0.95) in an initial burst stage, and then dramatically dropped down to the trough (0.3), which indicates the major burst stage. Meanwhile, the weight values for the CoM-feedback model subsystem (w_a) was, on the contrary, decreased to 0.3 in the initial burst stage, and then correspondingly increased to 0.7 showing the major burst stage. This means that the muscle stretch reflex model subsystem predominated the contribution in the initial burst region,

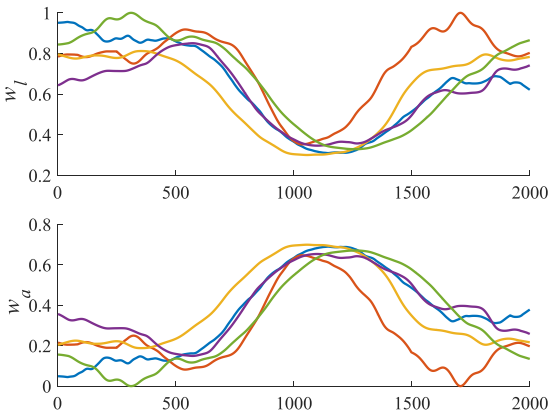

FIGURE 10. The weighting factors of contributing subsystems within the time course of 2s for each participant as represented in different colours. Sub-figure (a) represents the contribution of the muscle stretch reflex subsystem, and Sub-figure (b) represents that of the CoM-feedback model subsystem.

whereas the CoM-feedback model subsystem mainly works during the major burst region.

B. ENGINEERING SIMULATION APPROACH

The proposed artificial calf muscle activation model and the conventional muscle stretch reflex model were applied to a robotic ankle exoskeleton mounted on a human model for a comparative study, which was simulated using the OpenSim platform. Briefly, OpenSim is an open-source platform for modelling, simulating, and analysing musculoskeletal nerve control systems [35]. In this experiment, the simulated human model with a robotic ankle exoskeleton was applied to a standing control problem on a moving vehicle to evaluate the efficacy of the proposed artificial calf muscle activation model.

1) EXPERIMENTAL PROTOCOL

A 12 segment, 29 degrees-of-freedom (DOF) generic humanoid musculoskeletal model was adopted in this

work [15], [36]. The humanoid musculoskeletal model on a moving vehicle is illustrated in Fig. 11(a). The robotic ankle exoskeleton comprises two parts connected by a rotary joint, as shown in Fig. 11(b). The exoskeleton was mounted on the ankle of the human model as shown in Fig. 11(c) to provide movement assistance for the wearer.

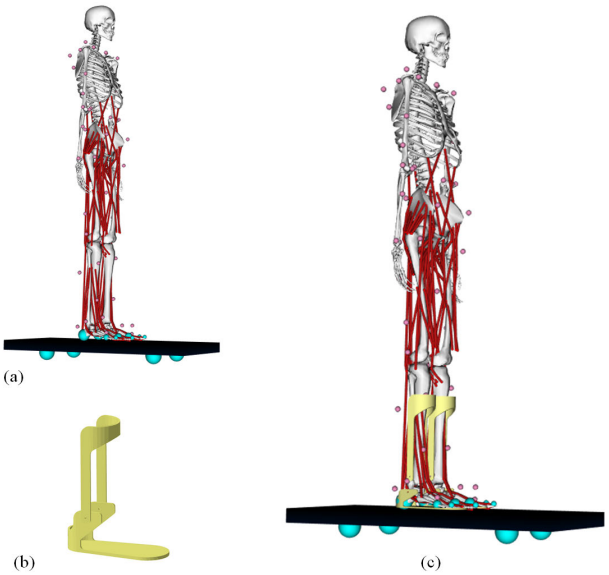

FIGURE 11. The simulated human model and the robotic ankle exoskeleton. (a) The humanoid musculoskeletal model. (b) The robotic ankle exoskeleton. (c) The exoskeleton mounted on the human model.

The parameters of the humanoid musculoskeletal module are listed in Table 1, where 'CoM' represents the vertical centre of the human body mass.

TABLE 1. Parameters of the human model.

Human model	Weight(kg)	Height(m)	CoM vertical(m)
Participant	75	1.75	1.09

In this simulation, the humanoid musculoskeletal model stood on a moving vehicle as shown in Fig. 11 (c) to perform upright standing control using the proposed artificial calf muscle activation model, where the vehicle was driven by an external force to simulate external disturbance. In particular, the ankle exoskeleton was driven by two calf muscle-tendon complex (MTC) models, i.e., the Gas MTC and Sol MTC, corresponding to the two calf muscles in the human ankle. The MTC model calculates the MTC force F_{MTC} according to the muscle activation, muscle spindle length l_m and its contraction velocity v_m, as expressed below:

$$F_{MTC} = aF^{\max} f_l(l_m) f_v(v_m), \tag{22}$$

where a denotes the MTC muscle activation, F^{max} is the maximum MTC force, $f_l(l_m)$ represents the force-length relationship function, $f_v(v_m)$ is the force-velocity relationship function of the Hill-type muscle model with more details can be found in [15]. The muscle spindle length l_m and its contraction velocity v_m can be calculated using the captured ankle angle, as detailed in Sec. III-B. Therefore, the only required parameter in MTC is the muscle activation; this was provided by the artificial calf muscle activation model proposed herein. To facilitate a comparative study, the conventional muscle stretch reflex model was also applied to provide the required muscle activation.

In this experiment, the vehicle was driven to move backward (the opposite direction of human faces) horizontally. The displacement was ranged between 0 and $0.15m$ as shown in Fig. 12(a); the velocity was ranged between 0 and $0.5m/s$ as shown in Fig. 12(b); the accelerations is ranged between $-1.7m/s^2$ and $-1.7m/s^2$ as shown in Fig. 12(c), as a simulation to usual vehicle movements in people's living environment; and the duration of vehicle moving is between $300ms$ and $900ms$ time points, as shown in Fig. 12(a)∼(c). The vehicle acceleration effectively produced a passive force to disturb the human upright balance in this experiment, and the proposed artificial calf muscle activation model would produce corresponding active force for the human model to balance the effect of the negative disturbance.

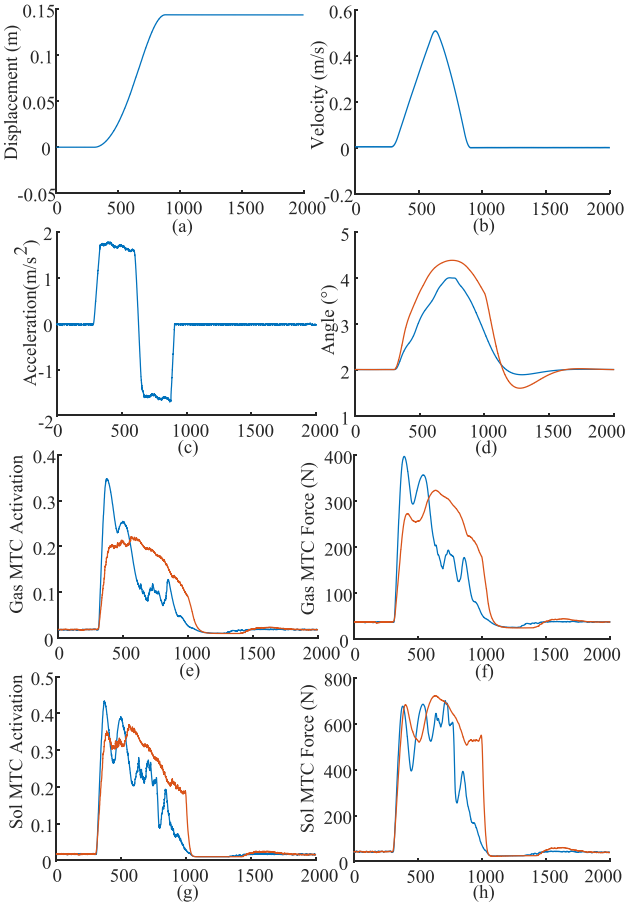

FIGURE 12. The vehicle kinematic information and the simulated response. In (d)∼(h), the blue solid lines represent the results led by the proposed approach, and the orange solid lines denote the results using the conventional muscle stretch reflex control.

2) EXPERIMENTAL RESULTS

The results based on the proposed artificial calf muscle activation model and the conventional muscle stretch reflex model, including human body tilt angle, Gas MTC and Sol MTC muscle activation, and the corresponding force, are illustrated in Fig. 12 (d)∼(h). Based on the muscle stretch reflex model, after the vehicle was imposed the force at time point 300*ms*, the human body leaned forward up to about 4.5° and then leaned backward to about 1.5°; the body was gradually stabilised at around 2.0°. In contrast, when the artificial calf muscle activation model control was applied, the human body leaned forward to about 4.0°, and then lean backward to about 1.9°, which is very close to the natural stabilised point around 2.0°. The change of the humanoid gravity led to some rotation torque; as a result, the MTC muscle activation based on both approaches was increased to produce corresponding MTC force to drive the robotic ankle exoskeleton to keep the body in the upright standing position.

Compared to the results led by the conventional muscle stretch reflex control, the leaned angle under the artificial calf muscle activation model control, in reference to the equilibrium position, is smaller, and the regulating process to equilibrium position is shorter. The reason is that the CoM-feedback subsystem in artificial calf muscle activation model control provided compensation for the MTC muscle activation. In specific, the calf muscle activation peak led by artificial calf muscle activation model control is larger than the peak under the conventional muscle stretch reflex control, as evidenced by Figs. 12 (e) and (g). Correspondingly, the MTC force peak is also larger under the artificial calf muscle activation model control, as shown in Figs. 12 (f) and (h). This suggests that the proposed artificial calf muscle activation model outperforms the conventional muscle stretch reflex model in controlling robotic ankle exoskeleton to assist human upright standing control. Noticing that exoskeleton may also be driven by the trajectories of joints, such as the work reported in [37], one piece of future work is to perform a comparative study between the two groups of approaches and investigate the combination of the two approaches for better performance.

V. CONCLUSION

This study proposed an artificial calf muscle activation model that provides a framework for simulating calf muscle activation during human upright standing control on a moving vehicle. The artificial calf muscle activation model is comprised by the muscle stretch reflex control model served as the LCNS and the CoM-based feedback model simulating the natural ACNS in the natural human calf. The proposed model was applied to a robotic ankle exoskeleton to assist wearers' movements. The results demonstrated that the calf muscle activation generated by natural mechanisms for human upright balance control on a moving vehicle can be predicted by the proposed artificial calf muscle activation model. The application of the proposed model was validated using a simulated exoskeleton in this work; it is interesting to apply the model to physical robotic exoskeleton control for more systematic evaluation and analysis.

REFERENCES

[1] M. Gomez-Ramirez, K. Hysaj, and E. Niebur, "Neural mechanisms of selective attention in the somatosensory system," *J. Neurophysiology*, vol. 116, no. 3, pp. 1218–1231, Sep. 2016.

[2] V. Stuphorn, "Neural mechanisms of response inhibition," *Current Opinion Behav. Sci.*, vol. 1, pp. 64–71, Feb. 2015.

[3] J. Iskander, M. Hossny, and S. Nahavandi, "A review on ocular biomechanic models for assessing visual fatigue in virtual reality," *IEEE Access*, vol. 6, pp. 19345–19361, 2018.

[4] M. Pang, X. Xu, B. Tang, K. Xiang, and Z. Ju, "Evaluation of calf muscle reflex control in the 'Ankle Strategy' during upright standing push-recovery," *Appl. Sci.*, vol. 9, no. 10, p. 2085, 2019.

[5] T. D. J. Welch and L. H. Ting, "A feedback model reproduces muscle activity during human postural responses to support-surface translations," *J. Neurophysiol.*, vol. 99, no. 2, pp. 1032–1038, Feb. 2008.

[6] T. D. J. Welch and L. H. Ting, "A feedback model explains the differential scaling of human postural responses to perturbation acceleration and velocity," *J. Neurophysiol.*, vol. 101, no. 6, pp. 3294–3309, Jun. 2009.

[7] K. Fujio, H. Obata, N. Kawashima, and K. Nakazawa, "The effects of temporal and spatial predictions on stretch reflexes of ankle flexor and extensor muscles while standing," *PLoS ONE*, vol. 11, no. 7, 2016, Art. no. e0158721.

[8] W. Taube, C. Leukel, and A. Gollhofer, "How neurons make us jump: The neural control of stretch-shortening cycle movements," *Exercise Sport Sci. Rev.*, vol. 40, no. 2, pp. 106–115, Apr. 2012.

[9] S. Song and H. Geyer, "Generalization of a muscle-reflex control model to 3D walking," in *Proc. 35th Annu. Int. Conf. IEEE Eng. Med. Biol. Soc. (EMBC)*, Jul. 2013, pp. 7463–7466.

[10] H. Geyer and H. Herr, "A muscle-reflex model that encodes principles of legged mechanics produces human walking dynamics and muscle activities," *IEEE Trans. Neural Syst. Rehabil. Eng.*, vol. 18, no. 3, pp. 263–273, Jun. 2010.

[11] K. Masani, A. H. Vette, and M. R. Popovic, "Controlling balance during quiet standing: Proportional and derivative controller generates preceding motor command to body sway position observed in experiments," *Gait Posture*, vol. 23, no. 2, pp. 164–172, Feb. 2006.

[12] J. P. Scholz, G. Schöner, W. L. Hsu, J. J. Jeka, F. Horak, and V. Martin, "Motor equivalent control of the center of mass in response to support surface perturbations," *Exp. Brain Res.*, vol. 180, no. 1, pp. 163–179, Jun. 2007.

[13] P. Jiang, R. Chiba, K. Takakusaki, and J. Ota, "Generation of the human biped stance by a neural controller able to compensate neurological time delay," *PLoS ONE*, vol. 11, no. 9, 2016, Art. no. e0163212.

[14] T. Mergner, "A neurological view on reactive human stance control," *Annu. Rev. Control*, vol. 34, no. 2, pp. 177–198, Dec. 2010.

[15] K. Yin, K. Xiang, M. Pang, J. Chen, P. Anderson, and L. Yang, "Personalised control of robotic ankle exoskeleton through experience-based adaptive fuzzy inference," *IEEE Access*, vol. 7, pp. 72221–72233, 2019.

[16] K. Tahboub and T. Mergner, "Biological and engineering approaches to human postural control," *Integr. Comput.-Aided Eng.*, vol. 14, no. 1, pp. 15–31, Jan. 2007.

[17] R. M. Enoka, *Neuromechanics of Human Movement*, 4th ed. Champaign, IL, USA: Human Kinetics, 2008.

[18] K. Takakusaki, M. Takahashi, K. Obara, and R. Chiba, "Neural substrates involved in the control of posture," *Adv. Robot.*, vol. 31, nos. 1–2, pp. 2–23, Jan. 2017.

[19] K. Nishikawa, A. A. Biewener, P. Aerts, A. N. Ahn, H. J. Chiel, M. A. Daley, T. L. Daniel, R. J. Full, M. E. Hale, T. L. Hedrick, A. K. Lappin, T. R. Nichols, R. D. Quinn, R. A. Satterlie, and B. Szymik, "Neuromechanics: An integrative approach for understanding motor control," *Integrative Comparative Biol.*, vol. 47, no. 1, pp. 16–54, 2007.

[20] M. Cenciarini and R. J. Peterka, "Stimulus-dependent changes in the vestibular contribution to human postural control," *J. Neurophysiol.*, vol. 95, no. 5, pp. 2733–2750, May 2006.

[21] M. J. Kang, C. S. Shin, and H. H. Yoo, "Modeling of stretch reflex activation considering muscle type," *IEEE Trans. Biomed. Eng.*, vol. 65, no. 5, pp. 980–988, Jul. 2017.

[22] N. Van der Noot, A. J. Ijspeert, and R. Ronsse, "Neuromuscular model achieving speed control and steering with a 3D bipedal walker," *Auto. Robots*, vol. 43, no. 6, pp. 1537–1554, Aug. 2019.
[23] M. F. Eilenberg, H. Geyer, and H. Herr, "Control of a powered Ankle–Foot prosthesis based on a neuromuscular model," *IEEE Trans. Neural Syst. Rehabil. Eng.*, vol. 18, no. 2, pp. 164–173, Apr. 2010.
[24] H. Geyer, A. Seyfarth, and R. Blickhan, "Positive force feedback in bouncing gaits?" *Proc. Roy. Soc. London. Ser. B, Biol. Sci.*, vol. 270, no. 1529, pp. 2173–2183, Oct. 2003.
[25] N. Thatte and H. Geyer, "Toward balance recovery with leg prostheses using neuromuscular model control," *IEEE Trans. Biomed. Eng.*, vol. 63, no. 5, pp. 904–913, May 2016.
[26] T. S. Buchanan, D. G. Lloyd, K. Manal, and T. F. Besier, "Neuromusculoskeletal modeling: Estimation of muscle forces and joint moments and movements from measurements of neural command," *J. Appl. Biomech.*, vol. 20, no. 4, pp. 367–395, Nov. 2004.
[27] D. A. Winter, *Biomechanics Motor Control Human Movement*. Hoboken, NJ, USA: Wiley, 2009.
[28] M. Venanzi, J. Guiver, P. Kohli, and N. R. Jennings, "Time-sensitive Bayesian information aggregation for crowdsourcing systems," *J. Artif. Intell. Res.*, vol. 56, pp. 517–545, Jul. 2016.
[29] G. Wei, H. Wang, X. Zhao, and R. Lin, "Hesitant triangular fuzzy information aggregation in multiple attribute decision making," *J. Intell. Fuzzy Syst.*, vol. 26, no. 3, pp. 1201–1209, 2014.
[30] Z. S. Xu and Q. L. Da, "An overview of operators for aggregating information," *Int. J. Intell. Syst.*, vol. 18, no. 9, pp. 953–969, Sep. 2003.
[31] L. Yang and Q. Shen, "Adaptive fuzzy interpolation," *IEEE Trans. Fuzzy Syst.*, vol. 19, no. 6, pp. 1107–1126, Dec. 2011.
[32] L. Yang, F. Chao, and Q. Shen, "Generalized adaptive fuzzy rule interpolation," *IEEE Trans. Fuzzy Syst.*, vol. 25, no. 4, pp. 839–853, Aug. 2017.
[33] K. Yin, M. Pang, K. Xiang, and C. Jing, "Optimization parameters of PID controller for powered ankle-foot prosthesis based on CMA evolution strategy," in *Proc. IEEE 7th Data Driven Control Learn. Syst. Conf. (DDCLS)*, May 2018, pp. 175–179.
[34] H. Hultborn, "Spinal reflexes, mechanisms and concepts: From eccles to lundberg and beyond," *Prog. Neurobiol.*, vol. 78, nos. 3–5, pp. 215–232, Feb. 2006.
[35] S. L. Delp, F. C. Anderson, A. S. Arnold, P. Loan, A. Habib, C. T. John, E. Guendelman, and D. G. Thelen, "OpenSim: Open-source software to create and analyze dynamic simulations of movement," *IEEE Trans. Biomed. Eng.*, vol. 54, no. 11, pp. 1940–1950, Nov. 2007.
[36] S. R. Hamner, A. Seth, and S. L. Delp, "Muscle contributions to propulsion and support during running," *J. Biomech.*, vol. 43, no. 14, pp. 2709–2716, 2010.
[37] R. Huang, H. Cheng, Y. Chen, Q. Chen, X. Lin, and J. Qiu, "Optimisation of reference gait trajectory of a lower limb exoskeleton," *Int. J. Social Robot.*, vol. 8, no. 2, pp. 223–235, Apr. 2016.

KAIYANG YIN received the M.E. degree from the Wuhan University of Technology, Wuhan, China, in 2015, where he is currently pursuing the Ph.D. degree. He is also a Visiting Ph.D. Student with the Department of Computer and Information Sciences, Northumbria University, Newcastle upon Tyne, U.K. His research interests include human motion signal analysis, bipedal robots control, and fuzzy logic systems.

JING CHEN received the B.E. degree from the Huazhong University of Science and Technology, Wuhan, China, in 1990, and the M.E. degree in industry automation and the Ph.D. degree in vibration control of civil engineering structure from the Wuhan University of Technology, Wuhan, China, in 1997 and 2003, respectively. She is currently a Full Professor with the School of Automation, Wuhan University of Technology. Her research interests include control science and engineering, computer control, power reactive power compensation, and harmonic suppression.

KUI XIANG received the B.E. degree from the Wuhan Technical University of Surveying and Mapping, Wuhan, China, in 1999, and the M.E. degree in mechanical dynamics and the Ph.D. degree in system sciences from Zhejiang University, Hangzhou, China, in 2002 and 2006, respectively. He is currently a Full Professor with the School of Automation, Wuhan University of Technology, Wuhan. His research interests include human motion signal analysis, modeling and statistical learning, and bipedal robots design and control.

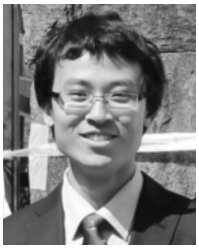

MUYE PANG received the Ph.D. degree in intelligent mechanical engineering from Kagawa University, Kagawa, Japan, in 2015. He is currently an Associate Professor with the School of Automation, Wuhan University of Technology, Wuhan, China. His research interests include neuromechanics, human–robot physical interaction, and robot actuator design and control.

BIWEI TANG received the Ph.D. degree in aircraft design from the School of Astronautic, Northwestern Polytechnical University, China, in 2018. He is currently a Lecturer with the School of Automation, Wuhan University of Technology, China. His current research interests include the optimization and control of human-exoskeleton interaction.

JIE LI received the Ph.D. degree in computer science from the Department of Computer and Information Sciences, Northumbria University, U.K., in 2018. He is currently a Lecturer with the School of Computing, Engineering and Digital Technologies, Teesside University, U.K. His research interests include computational intelligence, machine learning, intelligent decision-making systems, and cybersecurity.

LONGZHI YANG (Senior Member, IEEE) is currently the Director of Education and an Associate Professor with the Department of Computer and Information Sciences, Northumbria University, U.K. His research interests include computational intelligence, machine learning, big data, cyber security and privacy, computer vision, intelligent control systems, robotics, and the applications of such techniques under real-world uncertain environment. He is a Professional Member of the British Computer Society and a Senior Fellow of the Higher Education Academy, U.K. He received the Best Student Paper Award at the 2010 IEEE International Conference on Fuzzy Systems. He is the Founding Chair of the IEEE Special Interest Group on Big Data for Cyber Security and Privacy.